Photoabsorption Spectra of Alkali Cyanide Molecules in the Vacuum Ultraviolet Region

Hisato YASUMATSU, Tamotsu KONDOW,
Department of Chemistry, Faculty of Science, The University of Tokyo, Hongo, Bunkyo-ku, Tokyo 113, Japan
Kaoru SUZUKI, Kiyohiko TABAYASHI and Kosuke SHOBATAKE
Institute for Molecular Science, Myodaiji, Okazaki 444, Japan

It has been discovered in the collisional energy transfer from metastable rare gas atoms, $Ar(^3P_{2,0})$ or $Kr(^3P_{2,0})$, to alkali cyanide molecules, MCN (M=Na, K, Rb), that there exist two types of dissociative states, which lead to the M+CN($B^2\Sigma^+$) channel; one is a repulsive state and the other is a predissociative excited ion-pair state [1]. In order to obtain information on dissociative states, the photoaborption spectra of MCN in the energy range of about 6~11 eV were measured by use of BL-2A beam line.

Figure 1 shows an experimental set-up. A 1 m *Seya-Namioka* monochromator was used to monochromatize the synchrotron orbit radiation (SOR). An absorption cell containing a sample was heated up to 1000 K to maintain a vapor pressure of about 100 mTorr. The absorption cell was windowless; stainless steel capillaries with an inner diameter of 2 mm and a length of 30 mm were mounted at both ends of the absorption cell. Argon gas was blown onto the lithium fluoride window separating the measurement chamber from the SOR source so as to prevent the sample from depositing on it.

Panels (a) and (b) of Fig. 2 show the absorption spectra of NaCN and RbCN, respectively. The spectra consist of (1) peaks centering at 6.5, 8 and 10 eV with a fwhm of about 2 eV, (2) intense and broader structures, and other peaks. The energies of the peaks (1) were found to be almost independent of M, while the absorption edge of the broad structure (2) was red-shifted in parallel with the ionization potential of M, I_p[M].

Figure 3 shows the schematic potential enrgy curves of MCN. The repulsive portions of the potential energy curves are mimicked from those of MCl, because the electron affinity of CN is almost the same as that of Cl, and the ion-pair states are governed by the Coulomb interaction at a sufficiently large distance between M and CN, R_{M-CN}. The Franck-Condon transitions to the repulsive states give rise to the broad peaks with a fwhm of 1.5~2.5 eV. It is assigned, therefore, that the peaks of 6.5, 8 and 10 eV originate from the Franck-Condon transition to the repulsive states correlating to the M+CN(X), the M+CN(A) and the M+CN(B) channels, respectively. The other peaks correspond to the transitions to M*+CN(X, A and B) channels. On the other hand, the energies of ion-pair states are specifically dependent on M because of the I_p[M] difference as shown in Fig. 3. The intense and broad structures associated with the ion-pair states are explained in terms of thier high density of states [2] in this energy range. Our *ab initio* calculations of the potential energy curves of CN^- [3] shows that the density of states of $(CN^-)^*$ is very large in the energy range above 6 eV.

References

[1] H. Yasumatsu, K. Suzuki and T. Kondow, *to be published.*

[2] The density of states of excited ion-pair states, $M^+ \cdot (CN^-)^*$, is approximated to be given by that of $(CN^-)^*$.

[3] H. Yasumatsu, S. Iwata and T. Kondow, *to be published.*

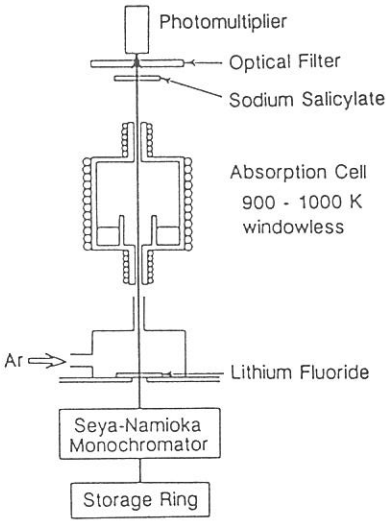

Figure 1: Schematic diagram of the apparatus.

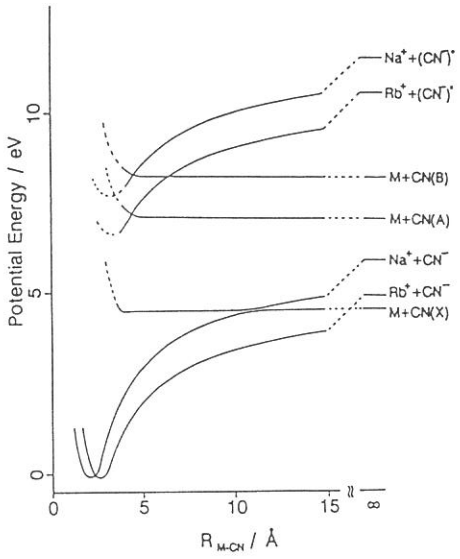

Figure 3: Schematic potential energy curves of MCN.

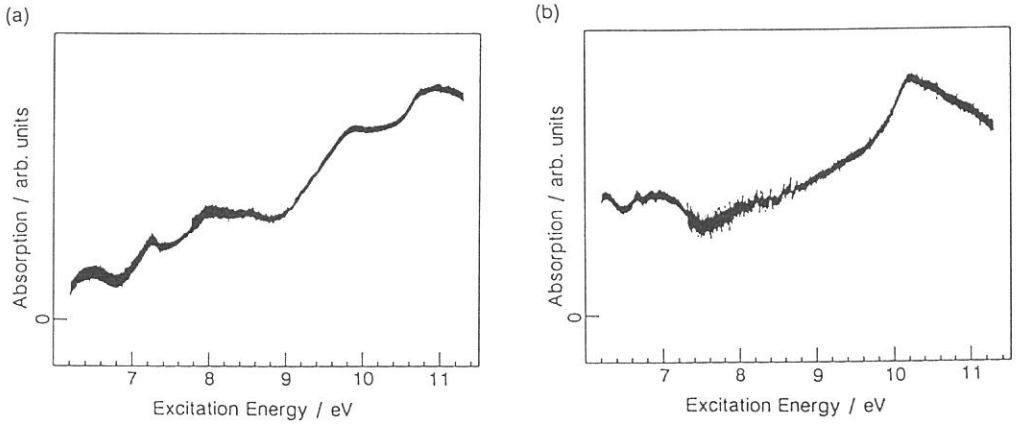

Figure 2: Absorption spectra of NaCN (panel (a)) and RbCN (panel (b)).

PHOTODISSOCIATION OF CYANOGEN IODIDE IN 105 - 175 nm REGION

Kazuhiro KANDA, Shunji KATSUMATA,
Takashi NAGATA*, Tamotsu KONDOW*,
Atsunari HIRAYA**, Kiyohiko TABAYASHI** and Kosuke SHOBATAKE**

Department of Fundamental Science, College of Science and Engineering, Iwaki Meisei University, Iwaki 970
* Department of Chemistry, Faculty of Science, The University of Tokyo, Bunkyo-ku 113
** Institute for Molecular Science, Myodaiji, Okazaki 444

When a cyanogen iodide (ICN) is photolyzed by a vacuum ultraviolet (VUV) radiation, a CN radical is formed in a variety of electronically excited states. The CN fragment produced in $A^2\Pi_i$ or $B^2\Sigma^+$ states immediately decays via radiative processes into the ground electronic state. In the present study, the quantum yields for the production of CN(A) and CN(B) in the photodissociation of ICN were determined in the wavelength range of 105 - 175 nm by monitoring the subsequent CN emission as a function of excitation energy. The measurement was performed at the BL2A station of UVSOR.

Figure 1 depicts the observed VUV absorption spectrum of ICN (upper panel) along with quantum yield curves for the CN^* production (lower panel). Those absorption bands are assignable to the Rydberg transitions.[1] While the yield curves show complex structures, close examination reveals following tendencies; (1) the curves have dips at the wavelengths where the absorption cross section reaches maxima, and (2) the two yield curves almost mimic each other. By considering the fact that the absorption spectrum has non-zero base line, the finding (1) indicates that underlying continuum makes contribution to the production of both CN(A) and CN(B). The finding (2) implies that CN(A) and CN(B) fragments are produced via identical precursor states of ICN, while the

branching fraction for the CN(A) production is 2-3 times larger than that for CN(B). The highest occupied molecular orbital of ICN, $2\pi(\pi_{C-N})$ bonding orbital, correlates to the 1π orbital of CN radical. Hence, the promotion of an electron from the 2π orbital possibly gives rise to a hole in the 1π orbital of the incipient CN radical, which asymptotically correlates to a free CN fragment in $A^2\Pi_i$ state. It is inferred from the orbital-correlation scheme that the underlying continuum is associated with transitions involving an configurational excitation of the 2π electron. The quantum yields decrease abruptly at ~114 nm as increasing the excitation energy. This sudden drop in the quantum yield is ascribed to the ionization process which starts to occur at 114 nm.

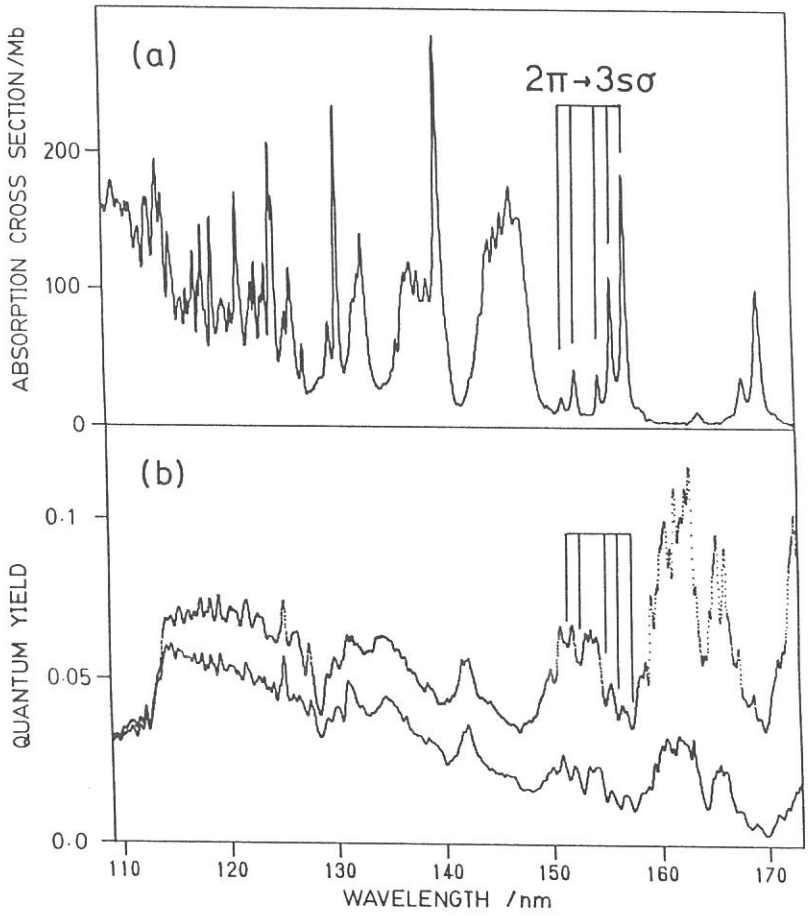

Fig. 1. (a) VUV absorption spectrum of ICN. (b) Quantum yield for the production of CN(A) (dotted line) and CN(B) (solid line) as a function of excitation wavelength.

[1] J. A. Myer and J. A. R. Samson, JCP, 52 (1970) 266.

Fluorescence Polarization of CN(B → X) Observed in Photodissociative Excitation of ClCN in the 105 - 145 nm Region

Mitsuhiko KONO, Kiyohiko TABAYASHI, and Kosuke SHOBATAKE

Institute for Molecular science, Myodaiji, Okazaki 444 Japan

Fluorescence polarization from $CN(B^2\Sigma^+)$ formed in photodissociative excitation process of ClCN was observed in the exciting wavelength region from 105 to 145 nm using synchrotron radiation as a polarized light source to study photodissociation dynamics. An absorption and fluorescence apparatus for vuv photochemical study constructed in the Beamline BL2A was used. The monochromated VUV light was introduced into a gas cell containing ClCN at 90 or 20 mtorr kept at room temperature. The intensity of the transparent light was measured in a conventional manner. The $CN(B^2\Sigma^+ \rightarrow X^2\Sigma^+)$ fluorescence emitted to the direction perpendicular to both the pointing vector and the polarization vector of the incident light. The degree of polarization for CN(B→X) fluorescence was measured using a Hinds' photoelastic modulator. The resolution was 0.10 nm for absorption and fluorescence excitation measurement and 0.30 nm for polarization measurement.

In order to facilitate the measurement of fluorescence polarization in a wide wavelength range the degrees of polarization were measured at reference wavelengths λ_{ref} = 125.4 and 133.0 nm, $P_{ref} = (I_{||} - I_{\perp})/(I_{||} + I_{\perp}) = 0.1270 \pm 0.0015$ and 0.0945 ± 0.0017, respectively, where $I_{||}$ and $I_{\perp}$ are the observed polarized fluorescence intensities parallel and perpendicular to the polarization vector of the incident light. At other wavelengths the fluorescence counts, $N_{||}$ and $N_{\perp}$ for parallel and perpendicular polarization to the electric vector were measured through two plate polarizers followed by each a photomultiplier tube (Hamamatsu R585) on a photon counting mode. The difference in the detection efficiencies for the two detectors were corrected for so that P_{ref} value determined using a photoelastic modulator agrees with the P_{ref} value with two polarizers, i.e. the degree of polarization at the reference wavelength, $P_{ref} = (N_{||} - cN_{\perp}) / (N_{||} + c\,N_{\perp})$, where c is the correction factor to be determined. Once the correction factor, c, is determined the degree of polarization at other wavelength than λ_{ref} is determined from $P = (N_{||} - c\,N_{\perp}) / (N_{||} + c\,N_{\perp})$, that is $I_{||} = N_{||}$ and $I_{\perp} = c\,N_{\perp}$ were adopted.

Figure 1 illustrates the degree of polarization for $CN(B^2\Sigma^+ \rightarrow X^2\Sigma^+)$ fluorescence, $P = (I_{||} - I_{\perp})/(I_{||} + I_{\perp})$, where $I_{||}$ and $I_{\perp}$ are the observed polarized fluorescence parallel and perpendicular to the polarization vector of the incident light against the wavelength of exciting light ranging in the region 105 nm to 145 nm. Figure 1 also shows absorption and fluorescence excitation spectra of ClCN gas in the cell. One finds that a) the degree of polarization is larger than 10 % above 111 nm and close to the limiting value of 1/ 7 and b) there appear undulatory structures around 116 nm and in the region from 120 to 126 nm. Compared with photodissociative excitation process of HCN and DCN molecules,[1] the dissociation seems to proceed via very short-lived

intermediates states, especially in the 117 - 130 nm region.

Since the sharp Rydberg progressions which appear in the 131 - 141 nm region are assigned to the transitions whose transition dipoles are perpendicular to the molecular axis, it is reasonable that the degrees of polarization become small at these peaks. However for the sharp Rydberg bands which appear in the 121 to 126 nm region and have been assigned to parallel transition, $4\sigma \rightarrow$ nsR the degree of polarization becomes smaller than the base values of polarization which is about P = 0.12. Probably the assignment should be changed from parallel to perpendicular transition.

Reference

1. K. Shobatake, A. Hiraya, K. Tabayashi, and T. Ibuki, *Vacuum Ultraviolet Photoionization and Photoemission of Molecules and Clusters*, Ed. by C. Y. Ng, (World Scientific Pub. Co., singapore, 1991) pp. 503-562.

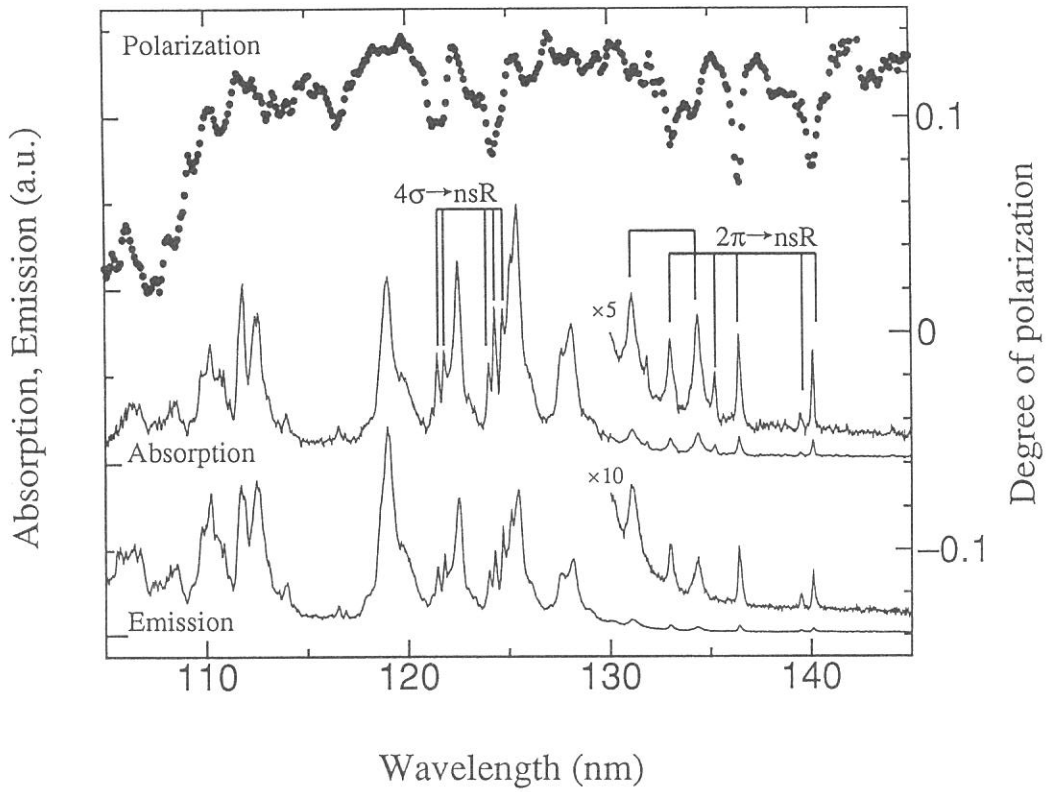

Figure 1. Absorption spectrum of ClCN, $CN(B^2\Sigma^+ \rightarrow X^2\Sigma^+)$ fluorescence excitation spectrum for the photodissociative excitation process $ClCN + h\nu \rightarrow Cl + CN(B^2\Sigma^+)$, and the degree of polarization $P = (I_{||} - I_{\perp})/(I_{||} + I_{\perp})$, plotted against exciting light wavelength ranging from 105 nm to 145 nm, where $I_{||}$ and $I_{\perp}$ are polarized fluorescence intensities parallel and perpendicular to the electric vector of the incident light. The resolution of the incident light for polarization measurement was 0.30 nm and 0.10 nm for the absorption and fluorescence excitation measurement.

Photo-induced Processes of Cl_2 ($1^1\Sigma^+_u$) State Studied by VUV/UV-Fluorescence Lifetime Measurements

Kiyohiko TABAYASHI,*† Mitsuhiko KONO,† Atsunari HIRAYA,*† and Kosuke SHOBATAKE*†

Institute for Molecular Science, and The Graduate University for Advanced Studies,† Myodaiji, Okazaki 444 Japan*

Photo-induced processes of excited Cl_2 in the presence of rare gas (Rg) third atoms are of fundamental importance in connection with our previous studies[1] on the excited state dynamics of Rg-Cl_2 van der Waals molecules generated in free jets. Here, VUV excitation light with a time duration of ca. 400 psec and a high repetition rate of 5.6 or 90.1 MHz (single-/multi-bunch operation of UVSOR) was successfully used for the time-resolved fluorescence measurements of Cl_2/Rg in a gas cell.

A typical time-decay curve for the fluorescence from ion-pair state of $Cl_2(1^1\Sigma^+_u)$ and that for excitation light are shown in **Figure 1**. The fluorescence for the bound-free transition $Cl_2(1^1\Sigma^+_u\text{-}X^1\Sigma^+_g)$ was collected in the region $185 < \lambda_{obs} < 215$ nm via a VUV monochromator and detected with a multichannel plate detector. Upon excitation to vibronic states ($1^1\Sigma^+_u$, $31 < v' < 41$) under the single collision condition (**Figure 2**), nearly a constant radiative decay of 2.65 nsec was obtained from a simple deconvolution analysis. **Figure 3** shows decay rates of Cl_2/Rg(Xe, Ne) system following λ_{ex}=137 nm excitation as a function of Rg partial pressure along with those of Cl_2/Ar case[2]. Collisional (total) quenching rate constants, $k(Xe) = 1.3\times10^{-9}$ and $k(Ne) = 1.4\times10^{-10}$ cm^3/sec are obtained. Since the reactive channel for $RgCl^*$ excimer formation is open only for Cl_2/Xe system in the excitation at $\lambda_{ex}\approx137$ nm, a comparable value of k(Xe) to k(Ar)= 9×10^{-10} cm^3/sec[2] indicates non-reactive collisional decays are quite effective for the excited ion-pare $Cl_2(1^1\Sigma^+_u)$ state. Relaxation to an intermediate $Cl_2(2^3\Pi_g)$ fluorescent state by collisional intersystem crossing is considered to be very important as one of the non-reactive quenching channels. Time-resolved fluorescence measurement for the $Cl_2(2^3\Pi_g)$ state as well as reaction product $XeCl^*(B)$ is under way to clarify the whole quenching mechanism of $Cl_2(1^1\Sigma^+_u)$ involved in Cl_2^*/Xe collision system.

References

[1] K. Shobatake, A. Hiraya, K. Tabayashi, and T. Ibuki, in *VUV Photoionization and Photodissociation of Molecules and Clusters*, C.Y. Ng ed. (World Sci.Pub. 1991), pp.503.

[2] T. Möller, B. Jordan, G. Zimmerer, D. Haaks, J. Le Calvé, and M.-C. Castex, Z. Phys. D **4**, 73 (1986).

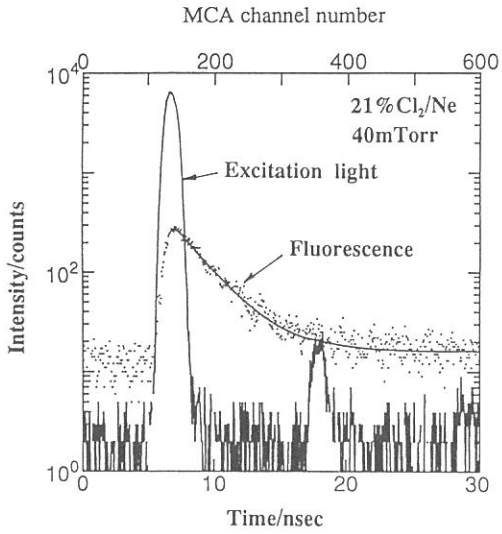

Figure 1. Time-decay profile for the $Cl_2(1^1\Sigma^+_u\text{-}X^1\Sigma^+_g)$ fluorescence upon excitation at 137nm and the time-profile of the scattered excitation light.

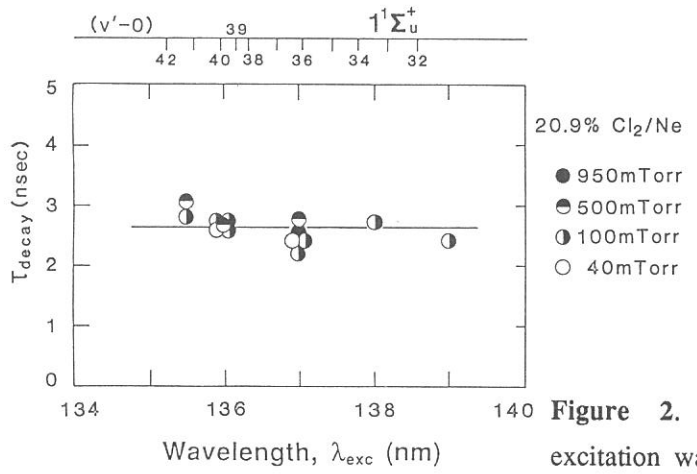

Figure 2. Radiative lifetime against excitation wavelength.

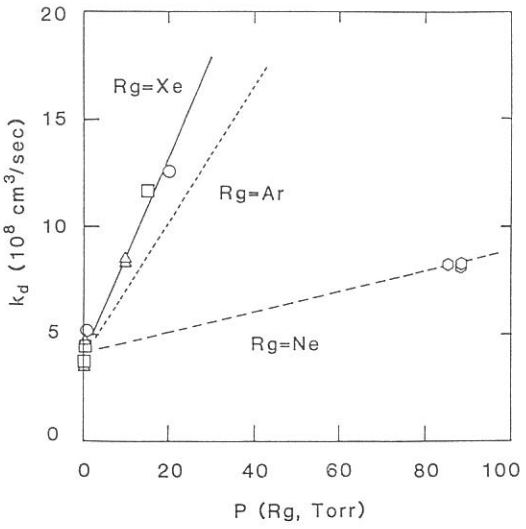

Figure 3. Decay rate for $Cl_2(1^1\Sigma^+_u\text{-}X^1\Sigma^+_g)$ fluorescence against Rg partial pressure upon excitation at 137nm.

PHOTOELECTRON SPECTRA OF ACETONE AND ACETONE DIMER

Kenji FURUYA,[1] Shunji KATSUMATA,[2] and Katsumi KIMURA[3]

[1]Institute for Molecular Science, Okazaki 444, and Department of Molecular Science and Technology, Kyushu University, Kasuga-shi, Fukuoka 816

[2]Department of Fundamental Science, Iwaki Meisei University, Iwaki-shi, Fukushima 970

[3]Institute for Molecular Science, Okazaki 444, and Japan Advanced Institute of Science and Technology, Tatsunokuchi, Ishikawa 923-12

In order to study the ionic states of acetone produced in a supersonic jet, we have carried out threshold photoelectron spectroscopy (TPES) with synchrotron radiation in the region 122.0 - 130.0 nm. Acetone has also been re-investigated with 58.4-nm He(I) photoelectron spectroscopy (PES). Figure 1 shows the PES [Fig. 1(a)] and the TPES [Fig. 1(b) and (c)] spectra. The energy resolutions are 21, 30, and 42 meV for spectra (a), (b), and (c), respectively. It has been found from Fig. 1 that the intensity of band 5 becomes stronger by lowering the resolution of the TPES analyzer. This fact cannot be explained in terms of the band broadening due to the lower resolution. Thus, we may conclude that there is an autoionizing state at 125.3 nm (9.893 ± 0.015 eV).

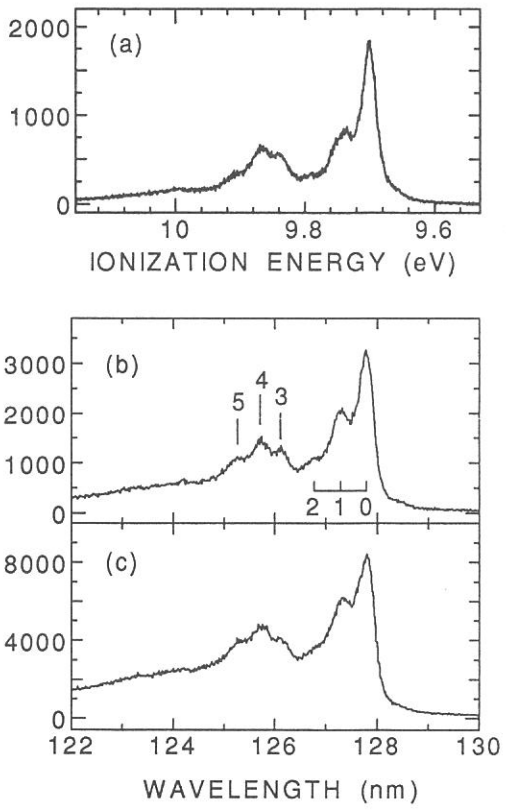

Fig.1 A He (I) photoelectron spectrum [(a)] and threshold photoelectron spectra [(b) and (c)] of acetone.

The threshold-photoelectron photoion coincidence (TPEPICO) spectra of acetone and its clusters were observed in the region 124.0 - 135.0 nm with an interval of 0.2 nm. A typical TPEPICO spectrum is shown in Fig. 2, observed at 131.0 nm (9.465 eV) which lies 0.235 eV below the adiabatic ionization potential of the acetone monomer (9.70 eV). The monomer cation peak in Fig. 2 is attributed to scattered light arising from some imperfection of the grating.

In the present experiments, the trimer and the tetramer cation intensities were much weaker than the dimer cation intensity (almost noise level) in all the observed TPEPICO spectra, as shown in Fig. 2. Thus, the contribution of larger clusters to the dimer cation peak observed in all the TPEPICO spectra is negligibly small. The solid curve in Fig. 3 was obtained by plotting the total dimer cation counts against the excitation wavelength, giving rise to intensity distribution corresponding to a TPES spectrum of the non-dissociative acetone dimer. The plotted curve may be called a 'TPEPICO excitation spectrum'. The

photoionization efficiency (PIE) curve of the dimer cation observed by Trott et al.[1] is shown in Fig. 3 by a dotted curve for comparison. From the TPEPICO excitation spectrum, the appearance ionization potential of the dimer cation has been evaluated to be 9.210 ± 0.015 eV. This value is slightly lower than that (9.26 ± 0.03 eV) evaluated by Trott et al.[1]

In the TPEPICO excitation spectrum shown in Fig. 3, there are two bands; one is a broad band with a peak at 129.6 nm, and the other is a satellite band with a peak at 127.2 nm. The latter peak position is identical to the PIE peak position. In contrast to the sharp vibrational bands of the monomer, the 129.6 nm band shows long tails, to either side of the band maximum implying that the potential minimum of the dimer cation is much different from that of the neutral dimer, and that the Franck-Condon factor of direct ionization is not zero for a very wide energy region.

The second electronic state of the acetone monomer cation is located at 12.59 eV (98.47 nm), much higher than the maximum positions, 9.747 eV (127.2 nm) and 9.567 (129.6 nm), observed in the present TPEPICO excitation spectrum. The difference is too large to explain the dimer production. Thus it is not expected that the two observed bands are related to the second electronic state of the acetone monomer. Since the upper state of the charge resonance states produced from the interaction between the two kinds of acetone dimer cations, acetone-$(acetone)^+$ and $(acetone)^+$-acetone in the electronic ground states, has a repulsive potential well, the upper state should not be observed in the present dimer TPEPICO excitation spectrum. The band shape observed at 127.2 nm in the PIE spectrum implies that this band cannot be due to the dimer cation. Therefore, we can conclude that the bands observed at 127.2 and 129.6 nm in the TPEPICO excitation spectrum are assigned to a Rydberg state of the neutral dimer and the electronic ground state of the dimer cation, respectively.

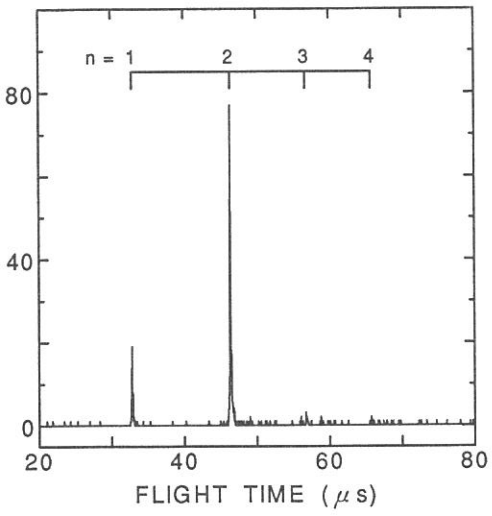

Fig.2 A threshold-photoelectron photoion coincidence (TPEPICO) spectrum of acetone clusters observed at 131.0 nm.

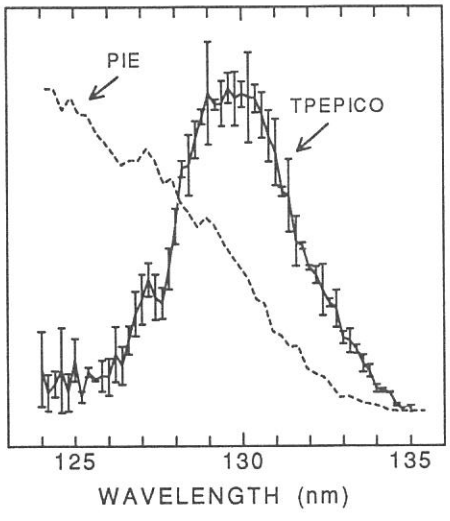

Fig.3 TPEPICO excitation (solid curve) and PIE (dotted curve) spectra of the acetone dimer. The PIE spectrum was taken from ref.[1].

[1]W. M. Trott, N. C. Blais, and E. A. Walters, *J. Chem. Phys.*, **69**, 3150 (1978).

IMPROVEMENT OF PHOTOELECTRON-PHOTOELECTRON COINCIDENCE SPECTROMETER AND AN INVESTIGATION OF DOUBLE IONIZATION PROCESSES BY EXCITATION ABOVE THE *3d* ELECTRON IONIZATION THRESHOLD REGION OF KRYPTON

Katsuhiko OKUYAMA, Eiken NAKAMURA, Kenji FURUYA[a], and Katsumi KIMURA[b]

Institute for Molecular Science, Okazaki 444

[a] Department of molecular science and technology, Kyushu Univ., Kasugashi Fukuoka 816

[b] Japan advanced institute of science and technology, Tatsunoguchi Ishikawa 923-12

Recently we have obtained successful results concerning a single-photon double-ionization process in Xe atom by means of a photoelectron-photoelectron coincidence (PEPECO) apparatus equipped with a magnetic-bottle time-of-flight (TOF) analyzer and the using the monochromatic orbiting radiation from the 25-pole undulator on beamline 3A2.[1] In order to expand our field of research to molecular systems as well as investigating a double-photoionization process in greater detail, we have initiated a series of improvements on the PEPECO apparatus. Firstly, we have introduced a new rear mirror that provides a suitable focal position for our apparatus, which has made the photon density 20-times higher than previously and has increased the coincident rate. Secondly, the photoelectron flight length of the short TOF tube constructed on the opposite side of the main TOF tube has increased from 4 cm to 14 cm and a small turbo molecular pump has been introduced to pump the short TOF tube. These improvements have resulted in a significant improvement in spectral resolution.

By using the PEPECO spectrometer improved, we investigated the double-ionization processes by photoexcitation just above the *3d* electron ionization threshold region of Kr atom. Fig. 1 shows the PEPECO spectrum of Kr atom at 124.5 A (99.6eV) with intensities recorded as dot density, of which horizontal and vertical axes show the times of flight on a linear scale in the short and long TOF analyzer, respectively. The excitation wavelength corresponds to 4.6 eV and 5.8 eV above $3d_{5/2}$ and $3d_{3/2}$ electron removal ionization threshold, respectively.[2] The double-cross structure observed on the spectrum clearly indicates that the double phtoionization process of Kr excited by 124.5 A single-photon chiefly occurs as indirect mechanism via two $3d^{-1}$ states. Direct double

ionization process, yielding the electronic ground terms of Kr^{+2}, is identified as minor process (20%) superimposing on the major double cross structure.

References

1) K.Okuyama, J.H.D.Eland, and K.Kimura, *Phys. Rev. A,* **41** 4930 (1990).

2) G.C.King, M.Tronc, F.H.Read, and R.C.Bradford, *J. Phys. B : Atom Molec. Phys.,* **10** 2479 (1977).

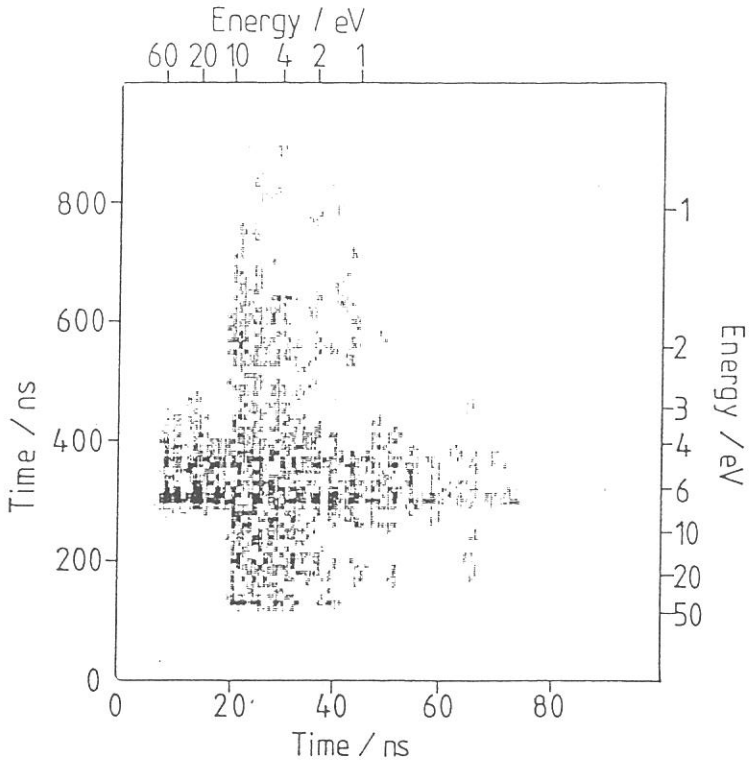

Figure 1 PEPECO spectrum of krypton at 124.5 A (99.6 eV) with intensities recorded as dot densities.

SINGLE AND DOUBLE PHOTOIONIZATION CROSS SECTIONS OF NO AND IONIC FRAGMENTATION OF NO^+ AND NO^{2+}

Toshio MASUOKA

Department of Applied Physics, Osaka City University, Sumiyoshi, Osaka 558

Single and double photoionization processes of nitric oxide (NO) have been studied in the photon energy region 37-100 eV by use of time-of-flight mass spectrometry and the photoion-photoion coincidence (PIPICO) method together with synchrotron radiation. The single (σ^+) and double (σ^{2+}) photoionization cross sections of NO are determined by a newly developed method.[1] The results are shown in Fig. 1 as a function of photon energy. The total cross section is from Ref. 2. It is emphasized that the double photoionization cross section reported in Fig. 1 includes both the dissociative and nondissociative processes of the precursor NO^{2+}. The threshold for the dissociative double photoionization was found to be 41.0 + 0.3 eV.

Ion branching ratios and the partial cross sections for the individual ions (NO^+, N^+, and O^+) produced from the precursor NO^+ and those (N^++O^+, NO^{2+}, N^{2+}, and O^{2+}) from NO^{2+} are also obtained.

The dissociation ratios of the singly and doubly charged precursors are shown in Fig. 2. It is interesting to note that the dissociation ratio of NO^{2+} reaches an asymptotic value very close to 0.85 at about 47 eV. The ground state of NO^{2+}, $X^2\Sigma^+$, is known to be nondissociative, and the first ($A^2\Pi$) and the second ($B^2\Sigma^+$) excited states to be partially bound. If only these bound states are the source for the (meta)stable NO^{2+}, the dissociation ratio should increase at higher photon energies. Obviously, the results in Fig. 2 provide an evidence for the presence of bound electronic states at higher photon energies and/or autoionization to the low-lying bound states of

NO^{2+}. On the other hand, the dissociation ratio of NO^+ decreases above 42.5 eV. This provably means that the Rydberg states converging to the low-lying electronic states of NO^{2+} are nondissociative and produce the (meta)stable NO^+. Above about 58 eV the dissociation ratio of NO^+ increases. However, the nondissociative process is still dominant even at higher photon energies. This strongly suggests that the majority of the high-lying electronic states of NO^+ are nondissociative.

References

1) T. Masuoka and H. Doi, Phys. Rev. A 1993, No. 1.

2) Y. Iida, F. Carnovale et al., Chem. Phys., 105, 211 (1986).

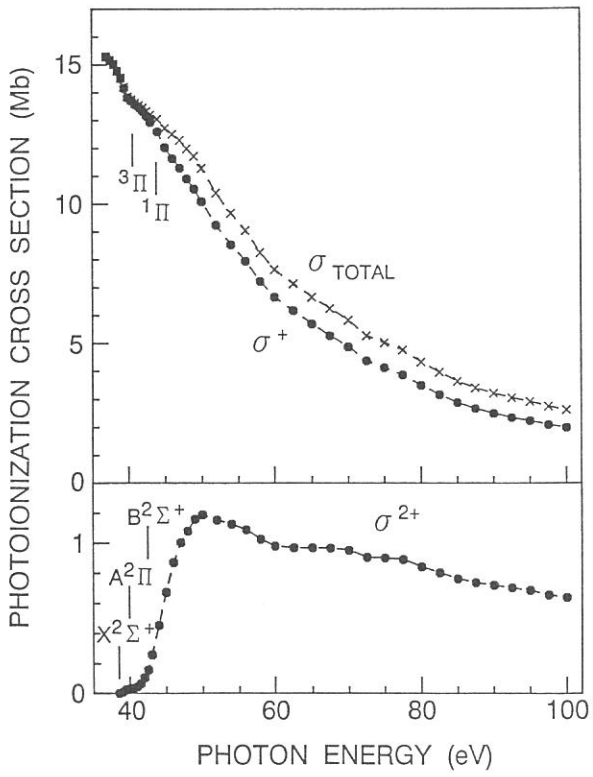

FIG. 1 Single (σ^+) and double (σ^{2+}) photoionization cross sections of NO.

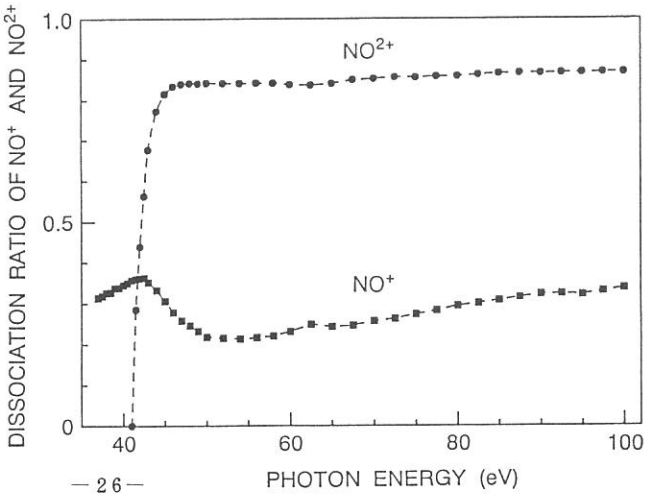

FIG. 2 Dissociation ratios of the precursors NO^+ and NO^{2+}.

DISSOCIATIVE MULTIPLE PHOTOIONIZATION OF BrCN AND ICN IN THE VALENCE SHELL AND n*d*(*n*=3,4) REGIONS

Toshio IBUKI, Inosuke KOYANO* and Toshio MASUOKA**

Kyoto University of Education, Fukakusa, Fushimi-ku 612
**Department of Material Science, Himeji Institute of Technology*
Kanaji, Kamigohri, Hyohgo 678-12
***Department of Applied Physics, Osaka City University, Sumiyoshi-ku, Osaka 558*

The multiple photoionization processes of BrCN and ICN in the valence and n*d* (n=3,4) inner shell region have been studied using photoion-photoion coincidence (PIPICO) techniques in the photon energy region of 40-130 eV at BL3A2 station of UVSOR. Figures 1 and 2 show the PIPICO branching ratios of the doubly charged BrCN and ICN, respectively, and those of the triply charged molecular ions are depicted in figs. 3 and 4. We can see some remarkable features from these figures:

(A) Doubly charged cation is formed by a single photon excitation of valence orbital electrons.

(A1) The decay channels of the doubly charged $BrCN^{2+}$ in fig. 1 change smoothly with increasing photon energy while those of ICN^{2+} are strongly affected at the ionization potential of $(4d)^{-1}$ as shown in fig. 2.

(A2) Neither (C^+ + N^+) nor (IC^+ + N^+) ion pair, which is formed in BrCN (see fig. 1), is observed in the ICN double photoionization.

(B) Triply charged ion precursors presumably arise primarily form double Auger decomposition processes of the initial n*d* hole states (see figs. 3 and 4).

(B1) The following three dissociation channels are observed for the triply charged cations: X^{2+} + CN^+ (1), X^{2+} + N^+ (2), and X^{2+} + C^+. (3)

(B2) The threshold energies of reactions (1)-(3) for X=Br are 70±1 eV, while for X=I the onset of reaction (1) is 59±1 and those of (2) and (3) lie 70±1 eV. The energy difference of about 10 eV between reactions (1) and (2) (and/or (3)) for X=I is very close to the bond energy of C≡N radical.

The above observations suggest that $BrCN^{2+}$ and $BrCN^{3+}$ seem to decompose explosively, while the multiply charged ICN may decompose successively.

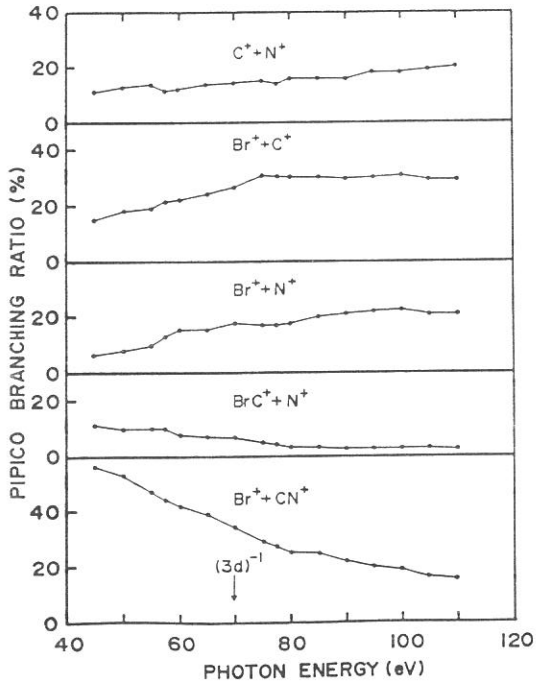

Fig.1. Photoionization branching ratios for doubly charged $BrCN^{2+}$.

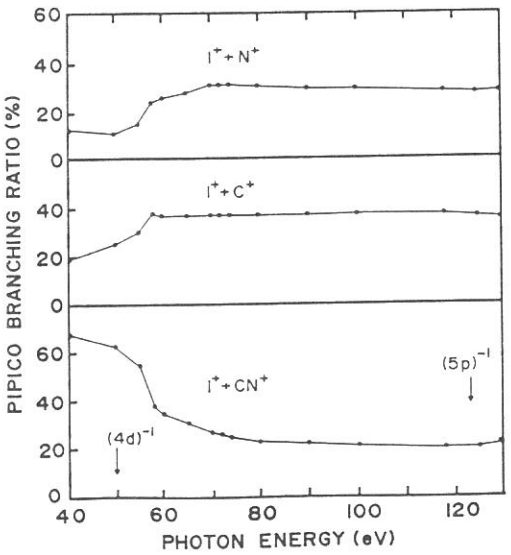

Fig.2. Photoionization branching ratios for doubly charged ICN^{2+}.

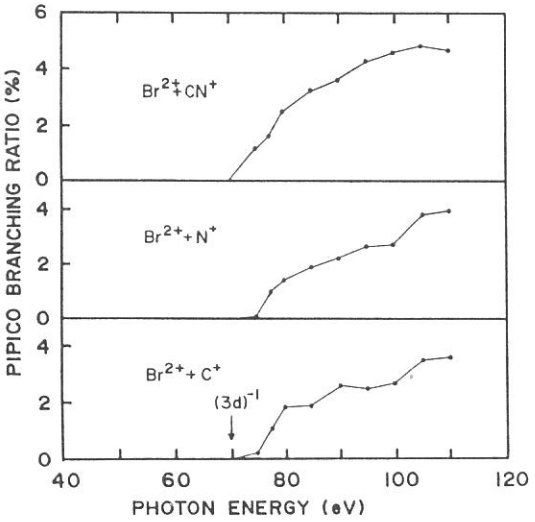

Fig.3. Photoionization branching ratios for triply charged $BrCN^{3+}$.

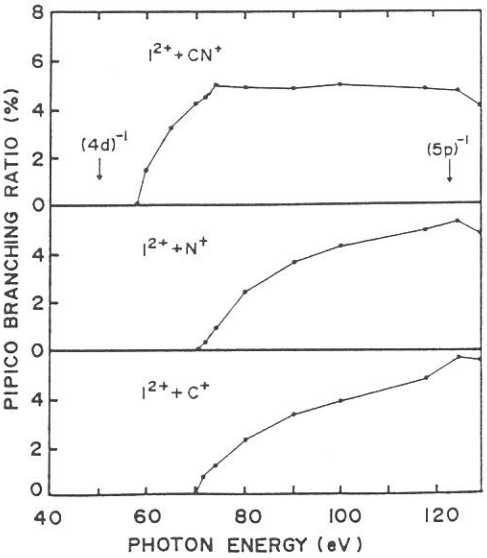

Fig.4. Photoionization branching ratios for triply charged ICN^{3+}.

Dissociation dynamics of SO^{2+} and CH_3F^{2+} studied by the triple photoelectron-photoion-photoion coincidence (PEPIPICO) method

Toshio Masuoka

Department of Applied Physics, Osaka City University,

Sumiyoshi-ku, Osaka 558

Multiple ionization of molecules has been extensively studied in recent years by using coincidence methods such as photoelectron-photoion (PEPICO), photoion-photoion (PIPICO), photoelectron-photoelectron (PEPECO), photoion-fluorescent photon (PIFCO), and photoelectron-photoion-photoion (PEPIPICO, or PE2PICO) coincidence.[1] These methods, which are essential to correlate two or more particles from each single ionization event, have provided much information on the multiple ionization of molecules. Among these, the PEPIPICO method has been shown to be a powerful technique to study the dissociation reactions of doubly and multiply charged molecules into three fragments.[2] Three-dimensional flight time distributions measured for dissociative double ionization clearly show the momentum distributions (speed and angle) of the fragments; thereby enabling determination of the charge separation mechanisms.

The dissociation dynamics of doubly and triply charged sulfur dioxide (SO_2) and methyl fluoride (CH_3F) are studied here by this technique over a photon energy region of 46-80 eV with the use of monochromatized synchrotron radiation. It was found that for the three-body dissociation of the type $ABC^{2+} \rightarrow A^+ + B^+ + C$, the dissociation mechanism is not dependent on the excitation energies in this region. This phenomenon suggests the presence of two site-specific positive holes each of which is related to a particular dissociation pathway. It is additionally concluded that atomization of the precursors is a dominant process in SO_2 at higher excitation energies.

Although several methyl compounds have recently been studied by the

PEPIPICO technique, the results for methyl fluoride have not yet been reported. Figure 1 shows a PEPIPICO distribution in the t_1 - t_2 plane at an excitation energy of 80 eV. Fourteen islands are observed, four of which have not been identified by previous PIPICO measurements.[3] The unidentified channels are CH_3^+, CH_2^+, CH^+, and C^+, each being in coincidence with F^+. It can be seen in Fig. 1 that the island size is very small in all the ionpair formations that include H^+ and H_2^+ ions; a result of the H^+ and H_2^+ ions taking almost all the energy but carrying very little momentum. Accordingly, it is difficult to obtain a definite slope for these islands and thus no analysis was made. The $CH_2^+ + F^+$ channel appears to be sequential via CH_3^+, since its slope is slightly less than 1. Similarly, the $H^+ + F^+$ channel has been suggested as being sequential via CH_3^+.[3] The $CH^+ + F^+$ and $C^+ + F^+$ channels are too weak to obtain meaningful island slope.

REFERENCES
1. J. H. D. Eland, Vacuum Ultraviolet Photoionization and Photodissociation of Molecules and Clusters, edited by C. Y. Ng (World Sci., Singapore, 1991), p. 297 and references therein.
2. J. H. D. Eland, F. S. Wort, and R. N. Royds, J. Electron Spectrosc. Relat. Phenom. **41**, 297 (1986).
3. T. Masuoka and I. Koyano, J. Chem. Phys. **95**, 1619 (1991).

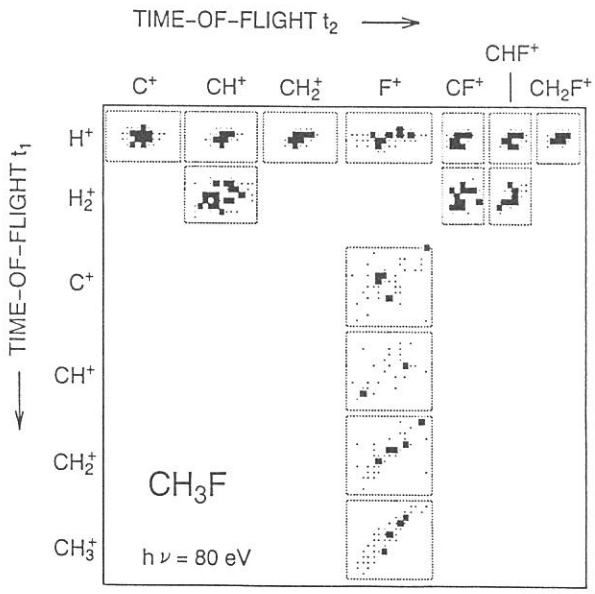

FIG. 1. TOF distributions for the dissociative double photoionization of CH_3F. Only a portion of each island is shown. Coincidences greater than 70% of the maximum intensity for each process are represented by solid rectangles; those greater than 40% and less than 70% are shown by dots.

IONIC FRAGMENTATION PROCESSES FOLLOWING Si:2p CORE LEVEL PHOTOEXCITATION AND PHOTOIONIZATION OF TETRACHLOROSILANE

Shin-ichi NAGAOKA, Toshio MASUOKA,[+] and Inosuke KOYANO[#]

Department of Chemistry, Faculty of Science, Ehime University, Matsuyama 790

[+]Department of Applied Physics, Osaka City University, Sumiyoshi, Osaka 558

[#]Department of Material Science, Faculty of Science, Himeji Institute of Technology, 1479-1 Kanaji, Kamigohri, Hyogo 678-12

In recent years, relaxation processes following core excitation and ionization in molecules have been a topic of much interest. We have investigated fragmentation following photoexcitation and photoionization of tetrachlorosilane (TCS) in the range of Si:2p excitation and ionization by means of the photoelectron-photoion and photoion-photoion coincidence methods (PEPICO and PIPICO methods, respectively).

The experiments were performed using a time-of-flight spectrometer with variable path length, coupled to a constant-deviation grazing incidence monochromator installed on the BL3A2 beam line of the UVSOR synchrotron radiation facility in Okazaki.[1]

The total photoionizaion efficiency curve of TCS has three peaks near the 2p core-ionization threshold of the silicon atom (Fig. 1). These peaks were assigned to the excitation of an Si:2p electron into $8a_1$, $9t_2$, and 4e orbitals below the threshold. There is an alternative interpretation (doubly excited state) for the peak seen at 110.1 eV. The Si:2p threshold of TCS is located at 110.17 eV. Resonant Auger processes follow the excitation at these peaks. Once an Si:2p core electron is initially excited (1 hole and 1 excited electron), the molecule is usually left with two holes in (a) valence orbital(s) and an excited electron in a virtual orbital. The two valence holes tend to fragment the system extensively.

Various ion pairs arise from Coulomb explosion processes from the dissociation of the unstable doubly charged ion.

Figure 2 shows an example of the photoionization mass spectra in the PEPICO mode. It was found that $I_{ion}/I_{tot\text{-}ion}$ for Si^+ and Cl^+ shows two broad peaks, one around 105 eV and the other around 110 eV. In contrast, $I_{ion}/I_{tot\text{-}ion}$ for all other ions decreases around these energies. It was also found that $I_{PIPICO}/I_{tot\text{-}PIPICO}$ for Si^+-Cl^+ shows pronounced peaks around 105 and 110 eV, whereas those for Cl^+-$SiCl_n^+$ (n = 1-3) show corresponding dips around these photon energies. The fragmentation scheme leading to the production of the ion pairs in TCS may be described as follows:

$$SiCl_4 + h\nu \rightarrow SiCl_4^{2+} + 2e \rightarrow Si^+ + Cl^+ + n.p.$$

1. T. Masuoka, T. Horigome, and I. Koyano, Rev. Sci. Instr. 60, 2179 (1989); E. Ishiguro, M. Suzui, J. Yamazaki, E. Nakamura, K. Sakai, O. Matsudo, N. Mizutani, K. Fukui, and M. Watanabe, Rev. Sci. Instr. 60, 2105 (1989).

Fig. 1 (left-hand side) Total photoionization efficiency curve of TCS in the range 100-115 eV.
Fig. 2 (right-hand side) Photoionization mass spectrum of TCS taken by excitation at 104.7 eV in the PEPICO mode.

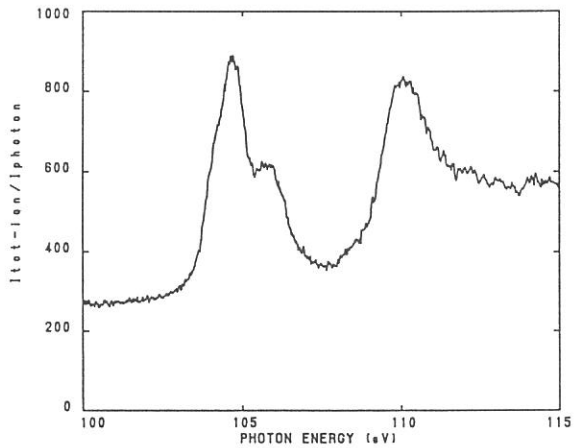

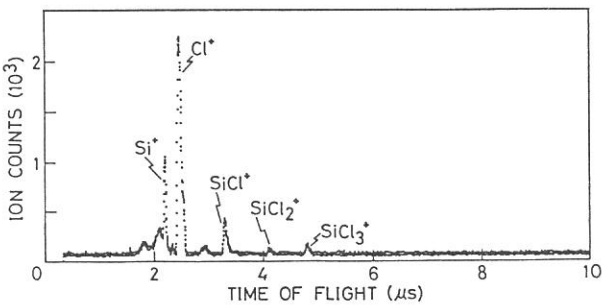

Dissociative Ionization Following Valence and Si:2*p* Core Level Photoexcitation of $HSi(CH_3)_3$ in the Photon Energy Range 24 - 133 eV

Bong Hyun Boo,[a] Inosuke Koyano,[b] Toshio Masuoka,[c] and Eiken Nakamura[d]

[a]*Department of Chemistry, Chungnam National University, Taejon 305-764, and Center for Molecular Science, 373-1 Kusung-dong Yusung-gu, Taejon 305-701, Korea*

[b]*Department of Material Science, Himeji Institute of Technology, 1479-1 Kanaji, Kamigohri, Hyogo 678-12*

[c]*Department of Applied Physics, Osaka City University, Sumiyoshi-ku, Osaka 558*

[d]*UVSOR, Institute for Molecular Science, Myodaiji, Okazaki 444*

Dissociation processes of $HSi(CH_3)_3$ have been investigated in the valence and Si:2*p* core-level photoionization by use of synchrotron radiation and the photoelectron-photoion coincidence (PEPICO) and photoion-photoion coincidence (PIPICO) techniques. Metastable $SiC_2H_n^{2+}$ is observed in the energy range E > 39 eV, respectively. Along with this dication, various monocations such as H^+, H_2^+, CH_n^+ (n=0-4) and $SiC_mH_n^+$ (m=0-3, n=0-9) are also observed. The ion branching and PIPICO ratios are measured as a function of the incident photon energy. Variation of the ion and the PIPICO branching ratios with the incident photon energy is shown in Figs. 1 and 2, respectively.

At the lowest energy examined, E = 24.00 eV, the most predominant process in the dissociative single photoionization of $HSi(CH_3)_3$ is the Si-C bond rupture forming $HSi(CH_3)_2^+$.

$HSi(CH_3)_3 + h\nu \rightarrow HSi(CH_3)_3^+ + e$ (valence ionization)

$HSi(CH_3)_3^+ \rightarrow HSi(CH_3)_2^+ + CH_3$

The ion branching ratio for H^+ rises beginning around 27 eV. Clear features are observed in the ion branching ratios for H^+ and H_2^+ in the energy ranges 95 < E < 110 eV and 100 < E <108 eV, respectively. Also in the PIPICO ratio data given in Fig. 2, processes 1, 2 and 3 are observed around 100 eV.

$HSi(CH_3)_3 + h\nu \rightarrow HSi(CH_3)_3^+ + e$ (Si:2*p* photoionization)

$HSi(CH_3)_3^+ \rightarrow HSi(CH_3)_3^{2+} + e$ (Auger) (1)

$HSi(CH_3)_3^{2+} \rightarrow CH_m^+ + SiC_nH_p^+$ (n=0-2) + n.p. (2)

$\rightarrow H^+ + SiC_nH_p^+$ (n=0-2) + n.p. (3)

where n.p. denotes the neutral products associated with the ionic products. Thus this energy corresponds to the Si:2*p* photoexcitation. In the range E > 100 eV, the source of CH_3^+ is mainly the dissociation channel, reaction 2. At energies beginning about 65 eV, the ion branching ratio of CH_3^+ slightly decreases. This decrease is correlated with the increase in the ion branching ratio of CH_n^+ (n=0-2). The core-level photoionization is observed to produce quite different fragmentation patterns showing the selective reactivities toward the Si-H and Si-C bonds giving rise to the bond cleavages. The core ionization of the localized Si:2*p* orbital results in the deposition of the internal energy to the silicon center, this internal

energy could be consumed to break the Si-H and/or Si-C bonds.

The valence double ionization and Si:2*p* core ionization thresholds are estimated to be ≈25 eV and 102 ± 1 eV, respectively. The Si:2*p* ionization threshold is similar to the $Si2p_{3/2}$ ionization energy of 111.6 eV in SiF_4.[1]

Reference

1. Aksela, K.; Tan, K. H.; Aksela, H.; Bankroft, G. M. *Phys. Rev. A 33*, **1986**, 258.

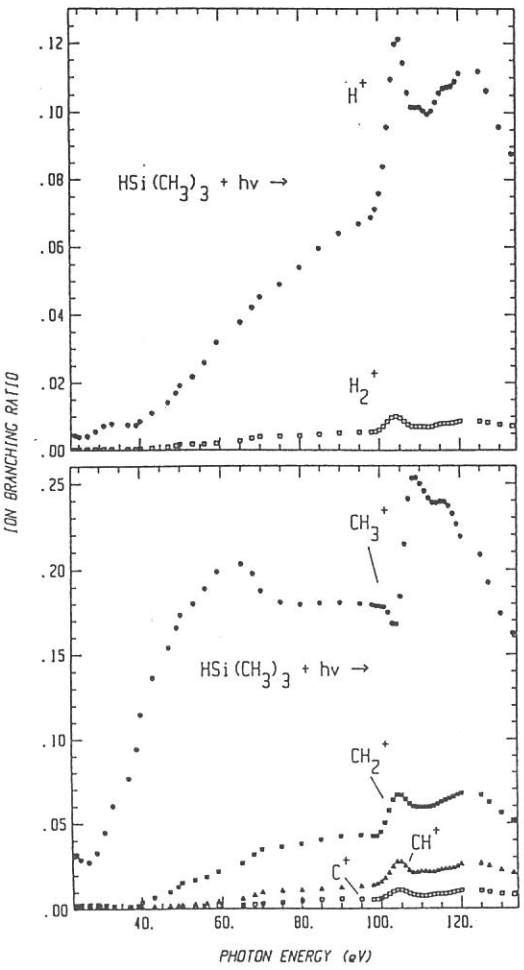

Figure 1. Ratios of integrated intensities of ion peaks in TOF mass spectrum to total photon intensity ($I_{ion}/I_{tot\text{-}ion}$) in $HSi(CH_3)_3$ as a function of photon energy.

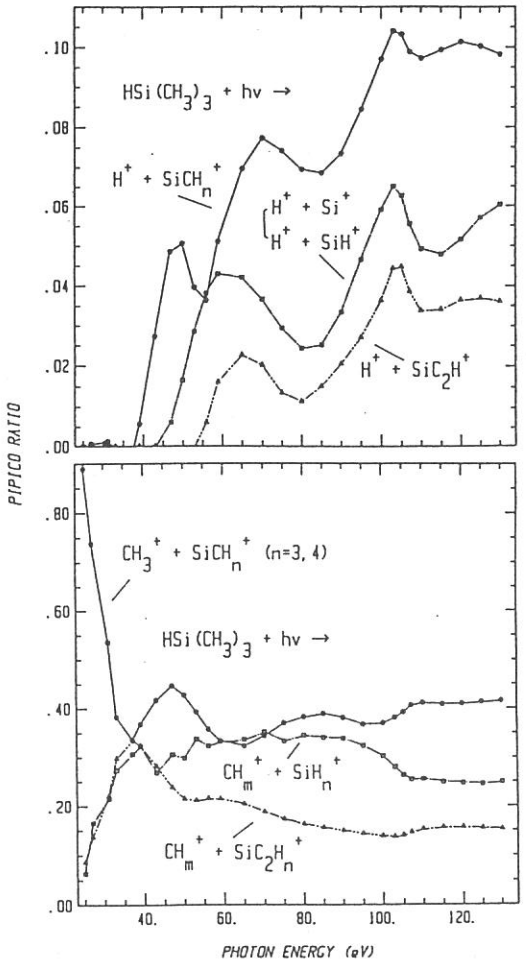

Figure 2. Ratios of integrated intensities of ion pairs in PIPICO spectrum to total double photo-ionization ($I_{PIPICO}/I_{tot\text{-}PIPICO}$) in $HSi(CH_3)_3$ as a function of photon energy.

POSITIVE ION-NEGATIVE ION COINCIDENCE SPECTROSCOPY OF O_2

Hiroaki YOSHIDA, Hideo HATTORI, and Koichiro MITSUKE

Department of Vacuum UV Photoscience, Institute for Molecular Science, Myodaiji, Okazaki 444

A new coincidence technique is developed for studying the ion-pair formation processes in the vacuum ultraviolet using synchrotron radiation. This technique utilizes the flight-time correlation of a pair of positive and negative ions produced by single photon excitation. The ion-pair formation from O_2 is studied for examining the performance of the apparatus.

Experiments are made by using synchrotron radiation emitted from beam line BL2B2 installed in the UVSOR storage ring. Figure 1 shows the schematic diagram of the time-of-flight mass spectrometer (TOFMS) and the data acquisition system. A sample gas is expanded into a beam expansion chamber from a nozzle of 100-μm diameter at room temperature of 298$\pm$3K and a stagnation pressure of 25 torr. The molecular beam is introduced through a conical skimmer into a photoionization chamber pumped to 10^{-6} torr when the beam is on. Ion pairs are formed by interaction with a monochromatized VUV photon beam at the photoexcitation region. Ion pairs thus produced are accelerated by an electrostatic field applied in the perpendicular direction to axes of both molecular beam and photon beam. Positive ions are mass-separated by a single-field type of TOFMS, while negative ions by a double-field type. The positive-ion signal is fed into the start input of a time-to-amplitude converter and the negative-ion signal into the stop input. Flight-time difference thus obtained is accumulated in a multichannel analyzer. Upon detection of a positive ion, a gate pulse voltage is applied to grid G2 to prevent electrons from penetrating the flight tube beyond G2. Application of this gate pulse is very effective in suppressing the false coincidence counts.

Figure 2 shows a coincidence spectrum of O^+ and O^- produced from O_2 at the photon wavelength of 709.5 Å (photon energy $E_{h\nu}$ = 17.47 eV). This energy is 0.2 eV distant from the threshold at 17.27 eV (717.8 Å) for the lowest ion-pair formation channel, $O_2(^3\Sigma_g^-) + h\nu \rightarrow O^+(^4S_u) + O^-(^2P_u)$. The background count is ascribed to the false coincidence signals, mainly arising from the start input of O_2^+ signals and the stop

input of electrons signals. The sharp peak observed at 14.22 μs is assigned to the coincidence peak due to the ion pairs produced by a single photoexcitation event. This assignment is supported by the following corroborating evidence. First, we clock the flight times separately for O^+ and O^- from photoexcitation region to the detectors by applying a pulse voltage to grid G2. The flight-time difference is estimated to be 14.4$\pm$0.5 μs, which is in good agreement with the position of the coincidence peak in Figure 2. Second, we measure the photodissociation efficiency curve for the ion-pair formation process by scanning the photon wavelength. This curve is compared with the efficiency curve of O^- measured by using molecular-beam photoionization apparatus on the beam line BL3B in the UVSOR facility. Several structures are commonly observed in the two curves.

Figure 1.

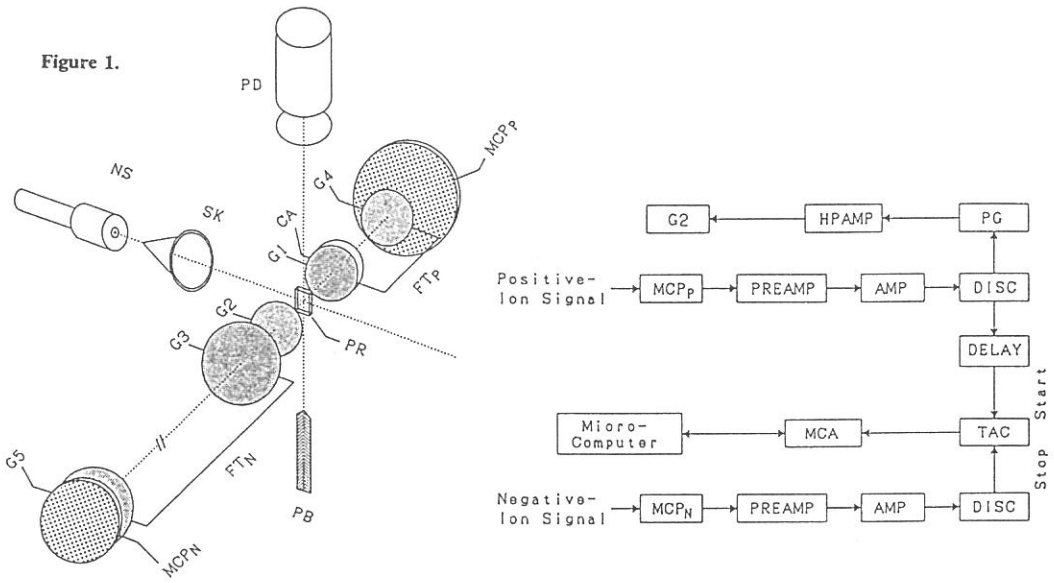

Figure 2.

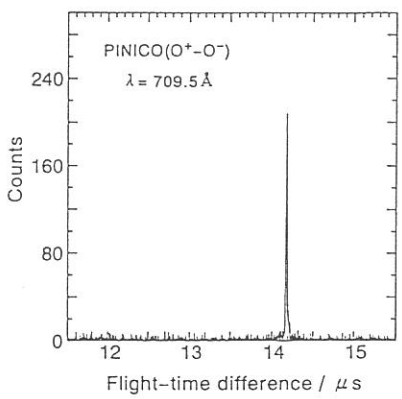

Figure 1. Schematic diagram of the time-of-flight mass spectrometers and data acquisition system for coincidence spectroscopy. (NS) nozzle source; (SK) conical skimmer; (PR) photoexcitation region; (PB) monochromatized photon beam; (PD) photon detector; (G1-G5) grids; (CA) capillary array plate; (FT_P) flight tube for positive ions; (FT_N) flight tube for negative ions; (MCP_P) microchannel plates for positive-ion detection; (MCP_N) microchannel plates for negative-ion detection; (PREAMP) pre-amplifier; (AMP) main-amplifier; (DISC) discriminator; (TAC) time-to-amplitude converter; (DELAY) delay circuit; (MCA) multichannel analyzer; (PG) pulse generator; (HPAMP) high-speed power amplifier.

Figure 2. Coincidence spectrum of O^+ and O^- produced from O_2 measured at the photon wavelength of 709.5 Å.

NEGATIVE-ION MASS SPECTROMETRIC STUDY OF ION-PAIR FORMATION IN THE VACUUM ULTRAVIOLET. $SO_2 \longrightarrow O^- + SO^+$, $O^- + S^+ + O$

Koichiro MITSUKE,[α] Shinzo SUZUKI,[β] Takashi IMAMURA,[γ] and Inosuke KOYANO[δ]

[α] Department of Vacuum UV Photoscience, Institute for Molecular Science, Myodaiji, Okazaki 444

[β] Department of Chemistry, Tokyo Metropolitan University, Minami-Osawa, Hachioji, Tokyo 192-03

[γ] Atmospheric Environment Division, National Institute for Environment Studies, Onogawa, Tsukuba, 305

[δ] Department of Material Science, Himeji Institute of Technology, 1479-1 Kanaji, Kamigohri, Hyogo 678-12

Photoexcitation of molecules to highly-excited states is often accompanied by dissociation into a pair of positive and negative ions in the photon energy range of 10 - 50 eV. The detection of negative ions produced by such ion-pair processes provides a sensitive probe to investigate the properties of Rydberg states lying in the vacuum ultraviolet. The present report describes ion-pair formation from photoexcitation of SO_2,

$$SO_2 + h\nu \longrightarrow O^- + SO^+, \quad (1)$$

$$SO_2 + h\nu \longrightarrow O^- + S^+ + O \quad (2)$$

studied by mass spectrometry using synchrotron radiation in the 15 - 35 eV photon energy range.[1] Negative ions O^- from SO_2 has been observed.

Figure 1 shows the O^- photodissociation efficiency curve. The appearance energy for O^- is in good agreement with the thermochemical threshold of 14.49 eV for the formation of $O^-(^2P_u) + SO^+(\tilde{X}\,^2\Pi)$. The cross section for process (1) at ~765 Å is estimated to be $(2.6\pm1)\times10^{-20}$cm^2 from a comparison between the count rate of O^- produced by process (1) and that of O^- produced from O_2. The quantum yield for process (1) is then obtained to be $(6.4\pm2.5)\times10^{-4}$ at ~765 Å from the total photoabsorption cross section for SO_2, 4.1×10^{-17}cm^2.

The efficiency curve can be divided into two regions: Region I [680 - 860 Å] containing sharp peaks, and Region II [370 - 680 Å] in which two broad peaks with maxima at ~610 and ~550 Å exist. The O^- efficiency rises markedly at the wavelengths of 622 and 570 Å . These onsets are attributed to the formation of triplets of fragments: $O^-(^2P_u) + S^+(^4S_u) + O(^3P_g)$ and $O^-(^2P_u) + S^+(^2D_u) + O(^3P_g)$. Region I appears to consist of a number of vibrational progressions which may be assigned to Rydberg states with

a variety of symmetry and principal quantum numbers. We can extract and assign three vibrational progressions in the symmetric stretching mode ν_1 for the *s*-type Rydberg states converging to SO_2^+ ($\tilde{D}\ ^2A_1$). Term values, effective principal quantum numbers, and quantum defects are calculated by using a Rydberg formula. Some of the vibrational progressions reported in the photoionization efficiency curve[2] of SO_2^+ from SO_2 are not discernible in our O^- efficiency curve. We can explain this discrepancy in terms of the specificity of the Rydberg states in the autoionization branching.

1) K. Mitsuke, S. Suzuki, T. Imamura, and I. Koyano, J. Org. Mass Spectrom. to be published.

2) J. Erickson and C. Y. Ng, J. Chem. Phys. **75,** 1650 (1981); C. Y. R. Wu and C. Y. Ng, J. Chem. Phys. **76,** 4406 (1982).

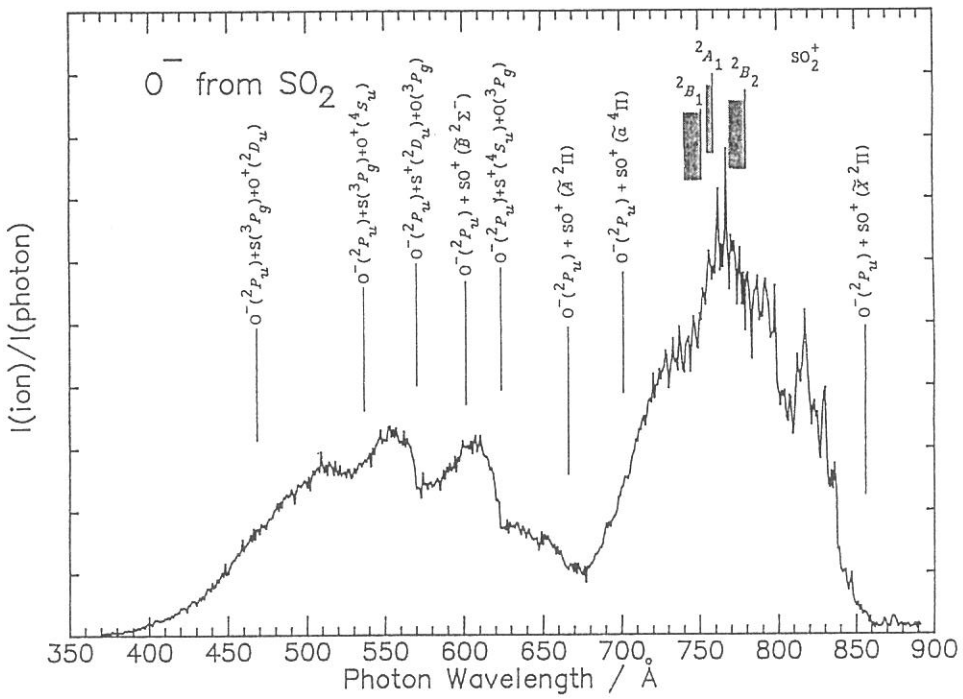

Figure 1. Photodissociation efficiency curve of O^- produced from SO_2 taken at a wavelength resolution (FWHM) of 0.8 Å and wavelength intervals of 1 Å. The vertical lines indicate the ionization limits for SO_2^+ ($\tilde{C}\ ^2B_2$, $\tilde{D}\ ^2A_1$, and $\tilde{E}\ ^2B_1$) and the thermochemical thresholds for possible ion-pair channels (Ref. 1).

ION-PAIR FORMATION FROM HYDROCARBONS BY PREDISSOCIATION OF RYDBERG STATES WITH C(2s)-HOLE CHARACTER

Hideo HATTORI, Hiroaki YOSHIDA, and Koichiro MITSUKE

Department of Vacuum UV Photoscience, Institute for Molecular Science, Myodaiji, Okazaki 444

Ion-pair formation induced by photoexcitation of saturated hydrocarbons ($RH+h\nu \rightarrow RH^{**} \rightarrow H^- + R^+$, $R=C_nH_{2n+1}$ n=1-5) has been studied by negative-ion mass spectrometry. We use monochromatized photon beam in the wavelength range of 400-1000Å at the beam line BL3B. All kinds of hydrocarbons are found to undergo predissociation into ion pairs with the cross section of 8.0×10^{-22} $-1.0\times10^{-20}cm^2$, when they are superexcited to Rydberg states formed by promotion of an electron in a molecular orbital composed of carbon 2s-type atomic orbitals.

Figure 1 shows the H^- photodissociation efficiency curve of ethane. Most of the peaks are assigned as resulting from transitions to the Rydberg states with C(2s)-hole character. A series of peaks observed in the energy range of 18.5-20.0eV correspond to vibrational progressions of the Rydberg states, $2a_{2u} \rightarrow$4s, 5s. We assign these peaks to the $v \geqq 0$ vibrational states of the ν_1(C-H stretching) and ν_3(C-C stretching) modes, as indicated in Fig.1(b), since their spacings are in good agreement with those for the $(2a_{2u})^{-1}$ band in He II photoelectron spectrum of C_2H_6.[1)]

Figures 2 and 3 show the photodissociation efficiency curves of H^- produced from propane and n-butane, respectively. Assignments of the Rydberg states which make peaks are indicated. We wish to point out that the ion-pair formation proceeds exclusively via the Rydberg states produced by promotion of a C(2s) electron. In all efficiency curves, there is not a peak over the whole energy range where the Rydberg states with excitation of an outer-valence electron are present. This finding can be interpreted as that other competitive decay pathways are dominant for these Rydberg states. Namely, Rydberg states with relatively lower excitation energies may have propensity to autoionize or predissociate into neutral fragments. Many molecular orbitals closely lie from -10 to -15eV, so that the energy widths for autoionization of such Rydberg states become large due to considerable overlap between the initially excited orbital and the target occupied orbital to be ionized.

As suggested by the efficiency curve of propane (Fig.2), predissociation into ion pairs

is markedly suppressed from the Rydberg states formed by promotion of an electron accommodated in the deepest inner-valence orbital, $3a_1$. Since this orbital has large overlap with the shallower $4a_1$ orbital, the lifetime of the Rydberg states converging to the $(3a_1)^{-1}$ ionic state is expected to be much shorter with respect to autoionization into the $(4a_1)^{-1}$ ionic state than with respect to conversion to the ion-pair state. Hence, these Rydberg states do not effectively predissociate into ion pairs in spite of their C(2s)-hole character. A similar phenomenon is observed for the Rydberg states of n-butane converging to the $(3a_g)^{-1}$ ionic state. (Fig.3)

1) J.W.Rabalais, and A.Katrib, Mol. Phys. 27, 923 (1974).

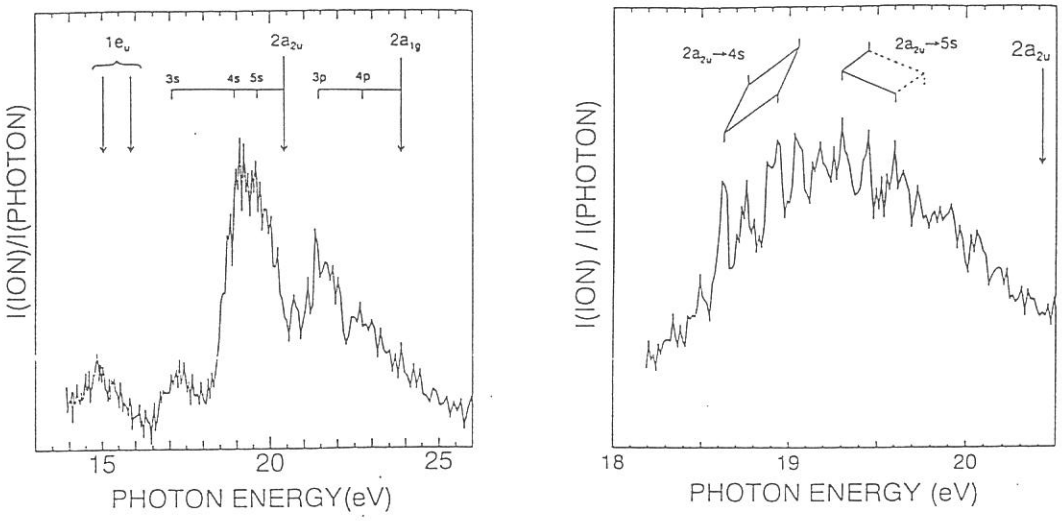

Figure 1 Photodissociation efficiency curves of H^- produced from ethane (a) with intervals of 2Å, and (b) with intervals of 0.5Å. The vertical IPs for molecular orbitals and assignments of the Rydberg states are indicated.

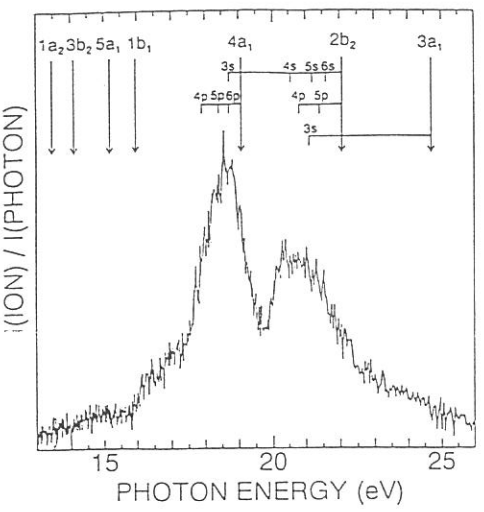

Figure 2 Photodissociation efficiency curves of H^- produced from propane.

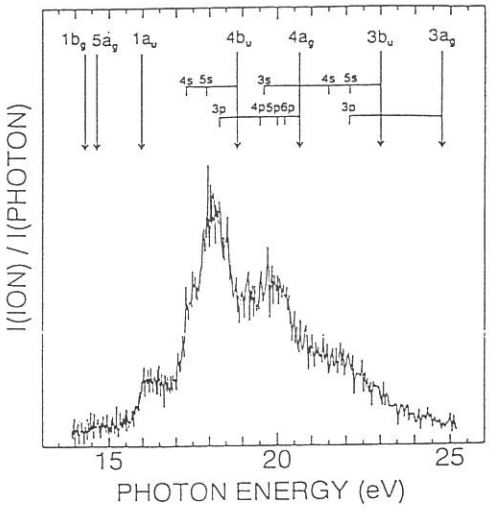

Figure 3 Photodissociation efficiency curves of H^- produced from n-butane.